Journal of Crystal Growth 692 (2026) 128675

Contents lists available at ScienceDirect

Journal of Crystal Growth

journal homepage: www.elsevier.com/locate/jcrysgro

Crystal growth kinetics and size-probability density function in phase transformations with spatially-correlated nuclei

Massimo Tomellini

Dipartimento di Scienze e Tecnologie Chimiche, Università di Roma Tor Vergata, Via della Ricerca Scientifica 1, 00133 Roma, Italy

ARTICLE INFO

Keywords:
Phase transition kinetics
Non-random nucleation
Crystal-size distribution function
Hard-sphere interaction
Kolmogorov-Johnson–Mehl–Avrami (KJMA) model

ABSTRACT

We present a study on crystal growth kinetics, nucleation kinetics and probability density function of crystal size, in nucleation and growth phase transformations with correlated nuclei. The method used is based on the theory of stochastic processes, for a set of correlated dots, that makes use of correlation functions. The theory is formulated within the framework of second-order approximation in correlation functions and is valid for any growth law of the crystals. It allows determining the rate of appearance of the actual nuclei, I_a, and the evolution of the mean crystal volume, v. The crystal-size distribution function is eventually computed using the I_a and v parameters. The model has been applied to a system of correlated nuclei according to the hard-sphere model in which the formation of actual nuclei is forbidden in a shell around growing crystals. The numerical results relating to 3D transformations are presented for linear crystal growth. This approach has also been used to describe uncorrelated nuclei (throughout the entire space) for which the exact solutions, for both I_a and v, are given by the Kolmogorov-Johnson-Mehl-Avrami (KJMA) theory. Comparison with the KJMA approach provides verification of the model's validity.

1. Introduction

Phenomenological models of the kinetics of phase transformations, governed by nucleation, growth and impingement between growing nuclei, often rest on the assumption that nucleation occurs randomly within the untransformed phase. In this context, the Kolmogorov Johnson Mehl Avrami (KJMA) mean-field theory was one of the first analytical approach, in terms of nucleation rate and growth law of nuclei, for determining the time evolution of the amount of the transformed phase [1–3]. Since its formulation, the theory's ability to describe phase transitions through analytical expressions has justified its widespread use in literature [4–9].

In this work we deal with phase transformations ruled by nucleation and growth with impingement that are of the KJMA-type. Hereafter, we refer to nucleation as the formation of the smallest stable cluster from which irreversible growth begins. In KJMA-type transition the critical size is considered nil, nuclei positions are fixed in space and upon collision between growing nuclei the mechanism of *impingement* comes into play. In the *impingement* mechanism, upon collision between growing nuclei (also referred to as crystals or grains) the growth ceases at the common interface without any redistribution of matter among them. On the contrary, in the *coalescence* mechanism a redistribution of matter occurs while conserving shape and mass. The modeling discussed in this paper applies, for instance, to primary recrystallization where nucleation, growth and grain impingement take place [4,9]. It does not, however, describe processes such as coarsening and Ostwald ripening. These transformations are driven by the gradient in surface energy between grains of different sizes, leading to the growth of large structures at the expense of smaller ones.

In KJMA-type transition, apart from the kinetics of the amount of the transformed phase, several experimental quantities have been modeled for the random case. These include the growth law of the actual crystals, the crystal size-probability density function (PDF) and the time evolution of the area of the interface between the new phase and the mother phase [10–12]. Approaches based on rate equations and continuous partial differential equations, such as the Fokker-Planck equations, are also used for determining the PDF [13–15]. However, quite often in several real systems the hypothesis of random arrangement of nuclei is not valid. For instance, this was ascertained in systems where progressive nucleation takes place at defect sites [16]. Also, progressive nucleation with diffusional growth, as in recrystallization and electrochemical phase formation, leads to a non-random distribution of nuclei [17–20]. This is due to a local depletion of supersaturation around growing nuclei, where nucleation is suppressed within a specific distance from their centers. It stems that the locations of nuclei are spatially correlated because the formation of a nucleus, at a given point of the space, affects the location of the other nuclei. The occurrence of non-Poissonian distribution of nuclei has also been investigated in non-solid-state transformations, specifically in those characterized by a coalescence mechanism. Statistical models on the reduction of

https://doi.org/10.1016/j.jcrysgro.2026.128675
Received 3 March 2026; Received in revised form 21 April 2026; Accepted 12 May 2026
Available online 15 May 2026

nucleation probability for a nearest droplet to an already formed one, have been investigated in ref.[21]. In ref. [22], the effect of supersaturation depletion due to bubble formation in decompressed fluids on the nucleation rate was studied. The authors developed a mean-field approach and introduced the concept an excluded volume where nucleation is suppressed – a concept that provided the basis of the model developed in the following sections.

The correlation function approach has proven to be a valuable tool for studying the effects of spatial correlation between nuclei in phase transformations by nucleation and growth with crystal impingement [23–26]. The stochastic approach makes use of probability functions given in terms of a series expansion in correlation functions. The rather low density of nuclei, when compared to the density of condensed phases, makes it possible to employ a truncation of the series up to second-order terms, yielding closed form solutions of the kinetics [23]. To the best of author's knowledge, the method on correlation functions has been applied to study the kinetics of the volume fraction of the transformed phase, the rate of formation of actual nuclei and the nearest-neighbor PDF of nuclei [23–27]. Aim of the present work is to complete the application of the method by computing the kinetics of growth of actual nuclei and the grain size PDF in phase transformations with correlated nuclei. By incorporating spatial correlation effects, the present stochastic approach captures physical features of the transformation that are intrinsically inaccessible to standard KJMA theory, such as those related to the growth law of nuclei, the nucleation rate, and the PDF. The analysis of these properties is central to the model developed here. Furthermore, the current approach enables the modeling of the phase transition up to its completion, providing a comprehensive kinetic description.

The paper is divided as follows: in section 2.1 we describe the stochastic approach for modeling the growth kinetics of actual crystals and the PDF of the crystal size. Section 2.2 is devoted to the application of the model to correlated nuclei according to the hard-sphere model and to the presentation of the numerical results. To make the subject matter easier to follow, most of the mathematical derivations are included in the Supplementary Material.

2. Results and discussion

2.1. General formulation

2.1.1. Growth kinetics of actual crystals

Phenomenological models of the kinetics of phase transformations can be expressed in terms of two quantities, that are given a priory, namely the law of crystal growth and the rate at which nuclei start growing. The growth law gives the time dependence of the grain radius, it is usually in the form of a power of time, $R \propto t^m$. Concerning the nucleation rate, two functions are defined: $I_a(t)$, that is the nucleation rate of actual nuclei (that can be measured in experiment) and $I_0(t)$, that is for the nucleation throughout the whole space including the transformed phase where actual nuclei cannot form. In the simplest case of random nucleation throughout the untransformed volume, the relationship between these rates is $I_a(t) = I_0(t)(1-\xi(t))$, with $\xi(t)$ volume fraction of the new phase. Consequently, $I_0(t)\xi(t)$ is the rate of formation of those "virtual" nuclei that lie in the transformed phase and do not contribute to the transformation. According to Avrami these nuclei are called phantoms. It is worth emphasizing that the importance of these nuclei is because, for random nucleation in space, the exact solution of the kinetics can only be obtained by using the nucleation rate including phantoms, $I_0(t)$ [3].

In phase transformations, the volume fraction of the transformed phase is identified as the probability that a generic point of the space belongs to that phase. Accordingly, stochastic approaches for the kinetics of phase transformations by nucleation, growth and grain impingement are based on computing the probability that no nuclei centers lie within a given domain centered at a generic point in space. In the following, we denote this domain with the symbol Δ and its measure, i.e. the volume, as $|\Delta| = \int_\Delta d\boldsymbol{r}$, Δ being the spatial integration domain.

In kinetics ruled by site-saturated nucleation and spherical nuclei, all nuclei start growing at $t = 0$, $I_0(t) = I_a(t) = n\delta(t)$ where $\delta(\cdot)$ is Dirac delta and n the number density of nuclei, all with the same radius. Let us denote with $\Delta(c, R(t))$ a spherical domain of radius $R(t)$ centered at a generic point in space, indicated by c, and with $Q_0(\Delta(c, R(t)))$ the probability that no nuclei centers are within the sphere of radius $R(t)$ centered at c. Also, let us consider $R(t)$ equal to the grain radius at t. The absence of nucleation centers in the sphere of radius equal to the grain radius at time t, ensures that the center of this sphere is not within any nucleus at that time, i.e. the generic point of the space, c, does not belong to the new phase at t. It follows that $Q_0(\Delta(c, R(t)))$ is the volume fraction of the untransformed phase; consequently $\xi(t) = 1 - Q_0(\Delta(c, R(t)))$ is the volume fraction of the transformed phase. For a random spatial distribution of nuclei, Q_0 is derived from the spatial Poisson process yielding $Q_0(\Delta(c, R(t))) = e^{-n|\Delta_t|}$, that is the KJMA kinetics for site-saturated nucleation [1], where the shorthand notation $\Delta_t = \Delta(c, R(t))$ has been used in the exponential argument.

In the case of progressive nucleation, we consider a collection of sets of nuclei with different birth times, $t_i \in [0, t]$ and number density n_i, where $i = 1, 2, \cdots, m$ and m is the number of sets. We denote with $\Delta(c, R(t_i, t))$ a spherical domain of radius $R(t_i, t)$ centered at c. Furthermore, we define the probability, indicated by $Q_0(t)$, that no nuclei of the classes $1, 2, \cdots, m$ lie in the spheres, $\Delta(c, R(t_1, t))$, $\Delta(c, R(t_2, t))$, …, $\Delta(c, R(t_m, t))$, respectively. Let $R(t_i, t)$ be the radius at time t of the grain belonging to the i-th class, i.e. with birth time t_i. It follows that $Q_0(t)$ is the probability that point c is not covered by any nucleus at t. Consequently, the probability that the point c belongs to the transformed phase is $\xi(t) = 1 - Q_0(t)$, namely the fraction of transformed volume.

For a random distribution of nuclei, the probability $Q_0(t)$ is given by $Q_0(t) = \prod_{i=1}^m Q_0(\Delta(c, R(t_i, t)))$, with $Q_0(\Delta(c, R(t_i, t)))$ being the probability that no nucleus of the i-th class lies within $\Delta(c, R(t_i, t))$. Use of the Poisson distribution provides $Q_0(t) = \prod_{i=1}^m Q_0(\Delta(c, R(t_i, t))) = e^{-\sum_{i=1}^m n_i |\Delta_{t_i,t}|}$ where the shorthand notation $\Delta_{t_i,t} = \Delta(c, R(t_i, t))$ has been used in the exponential argument. In the continuum limit, $n_i \to \frac{dn(\tau)}{d\tau} d\tau = I_0(\tau) d\tau$ and since $\xi(t) = 1 - Q_0(t)$ the KJMA kinetics is eventually obtained [1–3],

$$\xi(t) = 1 - \exp\left(- \int_0^t I_0(\tau) v_{ex}(t, \tau) d\tau \right), \tag{1}$$

with $v_{ex}(t, \tau) = |\Delta_{\tau,t}| = \gamma_D R(t-\tau)^D$ where D is the space dimension and γ_D a geometric factor ($\gamma_2 = \pi$, $\gamma_3 = 4\pi/3$). Owing to the random arrangement of nuclei the analytical solution Eq. (1) is given in terms of the nucleation rate including phantoms.

In Eq. (1), random nucleation in the entire space is considered which allows the use of Poisson process statistics. However, as reported in the Introduction, in phase transformations occurring in 2D and 3D space the random arrangement of nuclei is often the exception rather than the rule. In this case a valuable approach for modeling $Q_0(t)$ rests on the use of a series expansion in terms of either n-dots probability density functions (f_n) or n-dots correlation functions (g_n) [28,29]. With reference to the correlation functions method, truncation of the series up to second-order contributions provides the following expression for $Q_0(t)$,

$$Q_0(t) = \exp\left[- \int_0^t I_a(t_1) |\Delta_{t_1,t}| dt_1 + \int_0^t I_a(t_1) dt_1 \int_0^{t_1} I_a(t_2) dt_2 \int_{\Delta_{t_1,t}} d\boldsymbol{r}_1 \int_{\Delta_{t_2,t}} d\boldsymbol{r}_2 g_2(\boldsymbol{r}_1, \boldsymbol{r}_2, t_1, t_2) \right], \tag{2}$$

where $g_2(\boldsymbol{r}_1, \boldsymbol{r}_2, t_1, t_2)$ is the correlation function for a couple of nuclei with birth times t_1 and t_2 located at $\boldsymbol{r}_1$ and $\boldsymbol{r}_2$, respectively. To simplify

the expression, in Eq. (2) the shorthand notation $\Delta_{t_i,t} = \Delta(c, R(t_i,t))$ has been used for the integration domains. The pair-correlation function is linked to the radial distribution function through the relationship $g_2(\boldsymbol{r}_1, \boldsymbol{r}_2, t_1, t_2) = g(\boldsymbol{r}_1, \boldsymbol{r}_2, t_1, t_2) - 1$. In the following, we consider homogeneous systems for which the radial distribution function is a function of the relative distance $r = |\boldsymbol{r}_1 - \boldsymbol{r}_2|$. In Eq. (2), I_a is the actual nucleation rate. On one hand, considering the nucleation centers randomly distributed, it should be understood throughout the entire space, i.e. all nuclei including phantoms. In this case Eq. (2) reduces to the KJMA expression (Eq. (1)) by setting I_0 in place of I_a and $g_2 = 0$. In other words, Poisson statistics ($g_2 = 0$ in Eq. (2)) require a random distribution of nuclei and this is obtained by allowing nucleation throughout the whole space. On the other hand, the KJMA kinetics can also be obtained using Eq. (2) in terms of the actual nucleation rate, $I_a(t) = I_0(t)Q_0(t)$[1] by considering that actual nuclei are in fact spatially correlated (i.e. $g_2 \neq 0$) since nucleation of an actual nucleus is precluded in the transformed phase. Besides, for site-saturated nucleation the expression for the probability function is given by setting in Eq. (2) $I_a(t) = n\delta(t)$ and $g_2 = g_2(\boldsymbol{r}_1, \boldsymbol{r}_2)$ (see also the Supplementary Material for details). Clearly, in this case the concept of phantom nucleus loses meaning.

It is worth noting that Eq. (2) is quite general in that it gives the "empty space" probability for the domains $\Delta_{t_i,t} = \Delta(c, R(t_i,t))$ associated with the i-th class of nuclei. As reported above, to determine the volume fraction of the transformed phase, $R(t_i,t)$ is set equal to the nucleus radius at t. However, as discussed below, to determine the nucleation rate a different function could be used depending on the correlation function.

To determine the microscopic growth law of the grains and the crystal size PDF in the case of correlated nuclei, we define, at running time t, the PDF $f(v,t)$ such that $n_a(t)f(v,t)dv$ is the number density of grains with volume between v and $v + dv$, where $n_a(t)$ is the density of actual nuclei at t. We also define the "τ-crystal" PDF, $f_\tau(v,t)$, in such a way that $I_a(\tau)f_\tau(v,t)dvd\tau$ is the density of grains with volume between v and $v + dv$, at t, and with birth times between τ and $\tau + d\tau$ [10]. These two PDFs are linked through the expression

$$n_a(t)f(v,t) = \int_0^t I_a(\tau)f_\tau(v,t)d\tau. \tag{3a}$$

Furthermore, the volume fraction of the transformed phase is equal to $\xi(t) = n_a(t)\int vf(v,t)dv$. Substituting Eq. (3a) into this expression for $\xi(t)$ yields,

$$\xi(t) = \int_0^t I_a(\tau)\bar{v}(t,\tau)d\tau, \tag{3b}$$

where $\bar{v}(t,\tau) = \int vf_\tau(v,t)dv$ is the average volume of the "τ-crystal" population. In differential form Eq. (3b) reads ($\partial_t = \frac{\partial}{\partial t}$),

$$\partial_t\xi(t) = \int_0^t I_a(\tau)\partial_t\bar{v}(t,\tau)d\tau, \tag{3c}$$

where the boundary term is absent since $\bar{v}(t,t) = 0$.[2] Eq. (3c) is used for determining the relationship between $\bar{v}(t,\tau)$ and $v_{ex}(t,\tau)$. This is done employing the differential critical region approach developed by Alekseechkin [30] and the definition of the conditional probability $P_c(t|\tau)$ that is the probability that a generic point in space, say c, remains untransformed up to time t, given that an actual nucleus forms at time τ and at the distance $R(t-\tau)$ from c. The increment of the transformed volume fraction $d\xi(t)$ in time interval $(t, t + dt)$, due to an actual nucleation event occurring in time interval $(\tau, \tau + d\tau)$ reads: $d\xi(t) = P_c(t|\tau)[I_a(\tau)d\tau][\partial_t v_{ex}(t,\tau)dt]$. In fact, the term $\partial_t v_{ex}dt$ is equal to the volume element at distance $R(t-\tau)$ from c, and the product with the term $I_a(\tau)d\tau$ gives the number of τ-crystals capable of transforming c in the time interval dt at t, provided that c is untransformed up to t. This last condition is ensured by multiplying by the probability term $P_c(t|\tau)$. Integration of the previous equation with respect to τ yields

$$\partial_t\xi(t) = \int_0^t I_a(\tau)P_c(t|\tau)\partial_t v_{ex}(t,\tau)d\tau. \tag{4}$$

Equating Eqs. (3c) and (4) provides an equation for the $\bar{v}(t,\tau)$ unknown which admits as solution the following expression (see also the Supplementary Material),

$$\partial_t\bar{v}(t,\tau) = P_c(t|\tau)\partial_t v_{ex}(t,\tau). \tag{5a}$$

Integration of Eq. (5a) gives

$$\bar{v}(t,\tau) = \int_\tau^t P_c(s|\tau)\partial_s v_{ex}(s,\tau)ds, \tag{5b}$$

that is the basic equation for the mean volume of actual crystals that holds in the general case of correlated nuclei.

For KJMA compliant transformations the distribution of nuclei is random in the whole space and $I_a(\tau) = I_0(\tau)(1-\xi(\tau))$. As shown in the Supplementary Material section, in this case

$$P_c(t|\tau) = \frac{1-\xi(t)}{1-\xi(\tau)}, \tag{6}$$

that is the ratio between the unconditional probabilities that a generic point of the space is untransformed at t and at $\tau < t$. Therefore, for the average grain size in KJMA transformations Eq. (5b) becomes

$$\bar{v}(t,\tau) = \frac{1}{[1-\xi(\tau)]}\int_\tau^t [1-\xi(s)]\partial_s v_{ex}(s,\tau)ds. \tag{7}$$

For phase transformations with correlated nuclei the P_c probability has been determined in ref.[28] by using the series expansion of $\xi(t)$ in terms of f_n functions and comparing the $\partial_t\xi(t)$ derivative with Eq. (4). We remind that $[I_a(t_1)dt_1\boldsymbol{dr}_1][I_a(t_2)dt_2\boldsymbol{dr}_2]\ldots[I_a(t_n)dt_n\boldsymbol{dr}_n]f_n$ is the probability of finding nuclei born between t_i and $t_i + dt_i$ within the volume element $\boldsymbol{dr}_i$ at $\boldsymbol{r}_i$ irrespective of the position of the other $N-n$ nuclei, being N the total number of nuclei [29]. Next, the P_c probability is expressed in terms of correlation functions, g_n, by means of a cluster expansion of the f_n functions in terms of the g_n s. By retaining contributions up to second-order in correlation functions, the expression of $P_c(t|t_1)$ is eventually given by [28]

$$P_c(t|t_1) = \exp\left[-\int_0^t dt_2 I_a(t_2)\int_{\Delta_{t_2,t}} d\boldsymbol{r}_2\left(1 + g_2(\boldsymbol{r}_1, \boldsymbol{r}_2, t_1, t_2)\,|_{|\boldsymbol{r}_1|=R(t-t_1)}\right)\right], \tag{8}$$

where the spatial integral is performed over the $\Delta_{t_2,t}$ domain of measure $|\Delta_{t_2,t}| = \gamma_D R(t-t_2)^D$.

Eqs. (2),(5) and (8) are the main equations for modeling crystal volume and crystal-size distribution functions in the case of spatially correlated nuclei.

2.1.2. Crystal-size probability density function

The knowledge of both the $\bar{v}(t,\tau)$ function and the nucleation rate $I_a(\tau)$ allows determining the PDF for the crystal size, v, at running time t: $f(v,t)$. To this end, we defined the PDF for a single class of τ-crystals, i.e. with birth time between τ and $\tau + d\tau$, at time t: $f_\tau(v,t)$ [10]. In the case of KJMA-type transitions with progressive nucleation it was found that, as a first approximation, fluctuations can be neglected in the evolution equation for the $f_\tau(v,t)$ [14]:

$$\partial_t f_\tau(v,t) \cong -\partial_v(a_\tau(v,t)f_\tau(v,t)) \tag{9}$$

where $a_\tau(v,t)$ is such that $\partial_t\bar{v}(t,\tau) = \langle a_\tau(v,t)\rangle_v$ where the average value is taken over the f_τ-PDF. Neglecting fluctuations around the mean

[1] In this case Eq.(2) leads to an integral equation for $Q_0(t)$.

[2] In the framework of KJMA-like models, the size of the critical nucleus is assumed to be negligible.

size of "τ-crystals", in Eq. (9) we set $a_\tau(v,t) \cong \langle a_\tau(v,t)\rangle_v = \partial_t \bar{v}(t,\tau)$, to get

$$\frac{\partial f_\tau(v,t)}{\partial \bar{v}(t,\tau)} = -\frac{\partial f_\tau(v,t)}{\partial v}, \tag{10a}$$

with solution $f_\tau(v,t) = \phi(v - \bar{v}(t,\tau))$ where ϕ is defined by the initial condition on the distribution: $\phi(v - \bar{v}(\tau,\tau)) = \phi(v - v_0) = \delta(v - v_0)$ with v_0 initial size of the nucleus (in the following, $v_0 = 0$). The crystal-size PDF, Eq. (3a), yields

$$f(v,t) = \frac{1}{n_a(t)} \int_0^t I_a(\tau)\delta(v - \bar{v}(t,\tau))d\tau \tag{10b}$$

that is[3]

$$f(v,t) = \frac{1}{n_a(t)} \frac{I_a(\tau^*(t,v))}{\left|\frac{\partial \bar{v}(t,\tau)}{\partial \tau}\right|_{\tau=\tau^*(t,v)}}, \tag{10c}$$

where $\tau^*(t,v)$ is the root of the equation $v - \bar{v}(t,\tau^*) = 0$. Eq. (10c) gives the relation between the crystal-size PDF and the mean crystal volume, where the dispersion of the PDF is solely due to the nucleation process. In fact, for site-saturated nucleation a Delta-like PDF is attained: $f(v,t) \propto \delta(v - \bar{v}(t,0))$.

2.2. Application to time dependent hard-sphere correlation

2.2.1. Equations for $I_a(t)$ and $P_c(t|t_1)$

In this section, we apply the model to phase transformations by progressive nucleation and linear growth, when nucleation is prevented in a shell around growing nuclei. In this case, spatial correlation between nuclei can be modeled through a time dependent hard-sphere interaction where the pair distribution function for the couple of nuclei born at times t_1 and t_2 is given by $g(r,t_1,t_2) \cong H(r - r_c(t_1,t_2))$ where $H(\cdot)$ is the Heaviside step function and r_c the core radius. In fact, this expression for the $g(r)$ is an approximation that is obtained considering the first term of the cluster expansion of $g(r)$ [31]. However, as shown in [23] this is a good approximation for typical values of nucleation density in phase transitions.

Both hard-sphere and hard-disk pair-correlation models represent the simplest approaches to account for the suppression of nucleation in proximity of nuclei. This effect is caused by the depletion of local supersaturation in the mother phase due to nucleus growth. The hard-disk pair correlation function has been used to study the effect of the nucleation exclusion zone on electrodeposition kinetics, and to interpret experimental data on the spatial distribution of nearest neighbor nuclei [17,20]. As anticipated in the Introduction, similar approach has been applied to non-solid-state transformations [21,22], where the concept of an excluded volume – within which nucleation is suppressed- has been developed and mimics a hard-sphere interaction between nuclei.

In the present modeling, the correlation radius, r_c, is set equal to a sphere with radius greater than the grain radius by a constant length, β'. Accordingly, the distance between two *actual* nuclei that start growing at time t_1 and t_2 (with $t_1 > t_2$) cannot be shorter than $r_c(t_1,t_2) = R(t_1 - t_2) + \beta'$. The pair correlation function reads:

$$g_2(\boldsymbol{r}_1,\boldsymbol{r}_2,t_1,t_2) = H[|\boldsymbol{r}_1 - \boldsymbol{r}_2| - (R(t_1 - t_2) + \beta')] - 1. \tag{11}$$

The case $\beta' = 0$ relates to KJMA transformations described in terms of actual nucleation rate. In fact, as anticipated above, actual nuclei are spatially correlated since they only form in the untransformed phase. The formulation at $\beta' = 0$ is suitable to treat parabolic growth laws where Poisson statistics do not apply due to phantom overgrowth [30,32].

To evaluate the spatial integrals with correlation functions in Eqs. (2),(8), let us consider the integral $\int_{\Delta(R)} d\boldsymbol{r}_2 [H(|\boldsymbol{r}_1 - \boldsymbol{r}_2| - r_c)]$ where $\Delta(R)$ is a D-sphere of radius R. This integral has a geometrical interpretation: it is equal to the portion of the volume $|\Delta(R)|$ which lies outside the overlap volume between the spheres $\Delta(R)$ and $\Delta(r_c)$ at relative distance $r_1 = |\boldsymbol{r}_1|$. We denote this volume as $\omega[R, r_c; r_1]$. Consequently,

$-\int_{\Delta(R)} d\boldsymbol{r}_2 [H(|\boldsymbol{r}_1 - \boldsymbol{r}_2| - r_c) - 1] = (|\Delta(R)| - \omega[R,r_c;r_1]) = \overline{\omega}[R,r_c;r_1]$, namely the overlap volume of $\Delta(R)$ and $\Delta(r_c)$ at relative distance r_1 (see Fig. 1a).

As discussed above, the determination of the PDF requires the knowledge of both actual nucleation rate, $I_a(t)$, and $P_c(t|t_1)$ probability. As far as the actual nucleation rate is concerned, it is computed through Eq. (2) by solving the integral equation by successive iterations. In fact, for the hard-sphere correlation, at time t_1 an actual nucleus forms provided its distance from the center of another nucleus, already formed at $t_2 < t_1$, is greater than $R(t_1 - t_2) + \beta'$. By denoting with I_0 the nucleation rate throughout the whole volume where the transition occurs, we get

$$I_a(t) = I_0 Q_a(t), \tag{12}$$

where $Q_a(t)$ is the fraction of volume available for nucleation by considering correlation constraints. It follows that the computation of $Q_a(t)$ is equivalent to the solution of a phase transformation kinetics with growth law $r_c(t,\tau) = R(t - \tau) + \beta'$. To this purpose, one is tempted to employ the KJMA approach to estimate $Q_a(t)$. For linear growth it provides[4]

$$Q_{a,K}(\bar{t}) = e^{-(\bar{t}+\beta)^{D+1} + \beta^{D+1}}, \tag{13}$$

where dimensionless quantities, $\bar{t}$ and β were used (see section 2.3.2 and the Supplementary Material for details). However, KJMA kinetics does not provide the exact $Q_a(t)$ due to the presence of phantom nuclei, which is intrinsic to the Poisson process. In fact, the "growth law" $r_c(t,\tau) = R(t - \tau) + \beta'$ is not compliant with the KJMA approach due to phantom overgrowth (Fig. 1b).

The determination of $Q_a(t)$ can be done using Eq. (2) with $\Delta_{\tau,t}$ the sphere of radius $R(t - \tau) + \beta'$. Moreover, $g_2(\boldsymbol{r}_1,\boldsymbol{r}_2,t_1,t_2)$ is given by Eq. (11) and its spatial integral over $\boldsymbol{r}_2$ is equal to $-\overline{\omega}[R(t - t_2) + \beta', R(t_1 - t_2) + \beta'; r_1]$ as depicted in Fig. 2a. It follows that Eq. (2) becomes an integral equation for $Q_a(t)$ that can be solved by iterations. It should be noted that whenever nucleation occurs randomly throughout the untransformed volume, implying $\beta' = 0$ in Eq. (11), $Q_a(t) = 1 - \xi(t)$ holds. This relation is also valid for parabolic-type growths for which the KJMA model does not apply. In this case $\xi(t)$ can be computed by Eq. (2), that is an integral equation for $\xi(t)$.

Once the $I_a(t)$ nucleation rate has been determined, the transformed volume fraction, $\xi(t)$, can be calculated using Eq. (2) again. However, in this case $\Delta_{\tau,t}$ is the sphere or radius $R(t - \tau)$, $g_2(\boldsymbol{r}_1,\boldsymbol{r}_2,t_1,t_2)$ is given by Eq. (11) and its spatial integral over $\boldsymbol{r}_2$ is equal to $-\overline{\omega}[R(t - t_2), R(t_1 - t_2) + \beta'; r_1]$, as illustrated in Fig. 2b.

Concerning the $P_c(t|t_1)$ probability, it is computed by means of Eq. (8) where $\Delta_{t_2,t}$ is a sphere of radius $R(t - t_2)$. In this case the spatial integral over $\boldsymbol{r}_2$ is equal to $|\Delta_{t_2,t}| - \overline{\omega}[R(t - t_2), R(t_1 - t_2) + \beta'; R(t - t_1)]$, as shown in Figs. 2c,2d. Eq. (8) includes both cases $t_1 > t_2$ (panel c) and $t_1 < t_2$ (panel d). The fact that in this case the domain $\Delta_{t_2,t}$ is the sphere of radius $R(t - t_2)$ is due to the formulation of P_c that is obtained from the derivative of the $\xi(t)$ [28].

The complete expressions of $\xi(t)$, $P_c(t|t_1)$ and the integral equation for $Q_a(t)$ are reported in the Supplementary Material in terms of dimensionless variables.

[3] We employ the property of the δ distribution with a single root of the $g(z)$ function: $\delta(g(z)) = \frac{\delta(z - z_0)}{\left|\frac{dg}{dz}\right|_{z=z_0}}$ with $g(z_0) = 0$. In Eq.(10b), at given t, $\bar{v}(t,\tau) - v = 0$ has a single root being $\bar{v}(t,\tau)$ a monotonic function of τ.

[4] $Q_{a,K}(t) = e^{-V_{ex}(t)}$ where $V_{ex}(t) = \gamma_D I_0 \int_0^t ((t - \tau) + \beta')^D d\tau$.

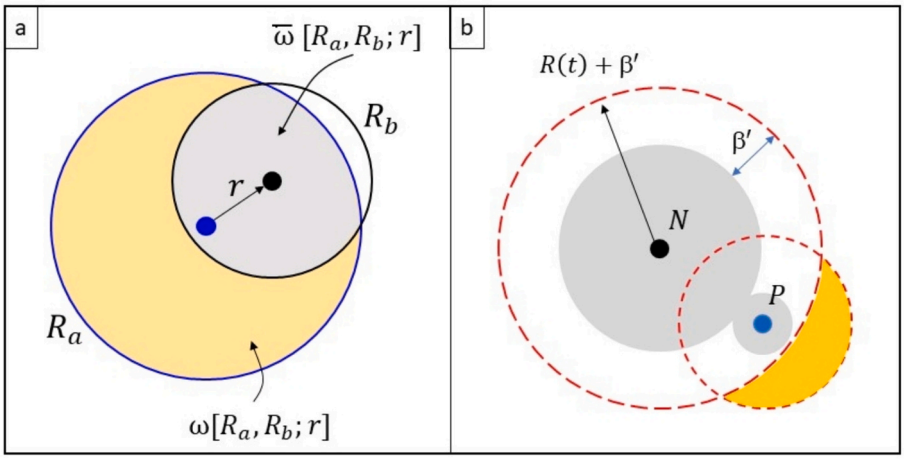

Fig. 1. Panel a): Graphical representation in 2D of the overlap area, $\overline{\omega}[R_a, R_b; r]$, between two disks of radius R_a and R_b at relative distance r (in gray). The area colored in yellow is equal to $\omega = \pi R_a^2 - \overline{\omega}[R_a, R_b; r]$. Panel b): Overgrowth of a phantom grain (P in the figure) in the KJMA approach for the growth law $r_c(t, t') = R(t - t') + \beta'$. In this case use of the KJMA model leads to an underestimation of the "untransformed" volume. In fact, the yellow portion of the "phantom" protruding from the actual grain (N in the figure) does not contribute to the actual transformation. (For interpretation of the references to colour in this figure legend, the reader is referred to the web version of this article.)

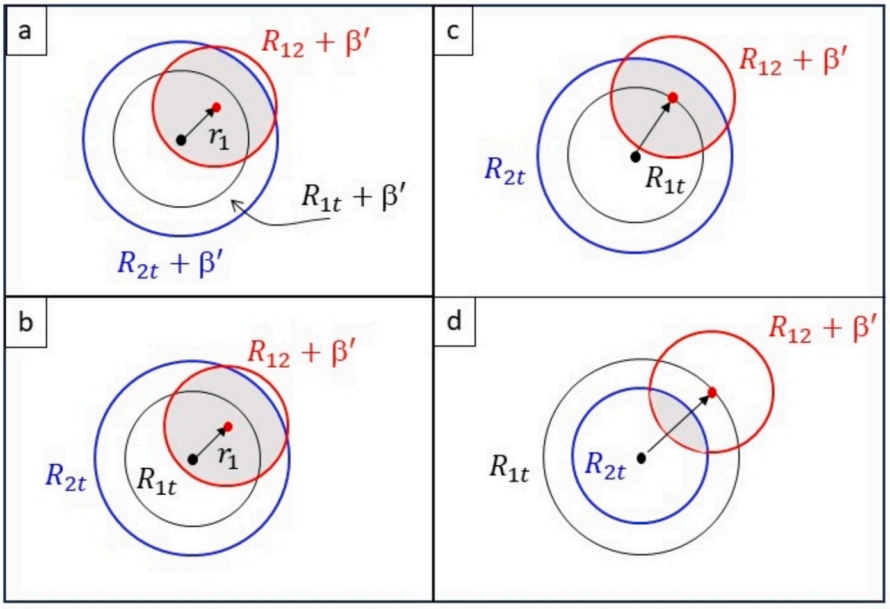

Fig. 2. Pictorial view, in 2D, on the geometrical meaning of the integral of the g_2 correlation function over the $\boldsymbol{r}_2$ space variable (Eq. (2) and Eq. (8)). In the figure, the short notations $R_{kt} = R(t - t_k)$ and $R_{12} = |R(t_1 - t_2)|$ were used. The overlap area (in gray) is linked to the integral of the correlation function that enters the computation of $Q_a(t)$ (panel a, Eq. (2)), $\xi(t)$ (panel b, Eq. (2)) and $P_c(t|t_1)$ (panels c,d, Eq. (8)). In Eq. (8) both cases $t_1 > t_2$ (panel c) and $t_1 < t_2$ (panel d) are to be considered.

Before concluding this section, we report the overlap volumes to be used in Eqs. (2) and (8) to model $\xi(t)$ and $P_c(t|t_1)$ in KJMA transformations with linear growth. As regards the computation of $\xi(t)$ using Eq. (2), since in this case $\beta' = 0$ and $R(t_1 - t_2) = R(t - t_2) - R(t - t_1)$, Figs. 2a-b show that the correlation sphere (with radius $R(t_1 - t_2)$) is within the integration domain $\Delta_{t_2,t}$ (sphere of radius $R(t - t_2)$). It follows that $\overline{\omega}[R(t - t_2), R(t_1 - t_2); r_1] = \gamma_D R^D(t_1 - t_2)$. Similarly, with regard to the computation of P_c, Fig. 2c shows that $\overline{\omega}[R(t - t_2), R(t_1 - t_2); R(t - t_1)] = \gamma_D R^D(t_1 - t_2)$, for $t_1 > t_2$ while $\overline{\omega}[R(t - t_2), R(t_2 - t_1); R(t - t_1)] = 0$, for $t_1 < t_2$.

2.2.2. Numerical results

In this section we report numerical outputs on the nucleation rate of actual nuclei, the growth kinetics of the crystals and the PDF of crystal size in progressive nucleation of correlated nuclei. We consider the cases of linear growth in 3D space and hard-sphere correlation. All the numerical calculations were performed using the Wolfram Mathematical package. The results are presented in terms of reduced time, namely $\bar{t} = \eta t$ with $\eta = \left(\frac{\pi I_0 G^3}{3}\right)^{1/4}$ and reduced volume $\nu = \overline{v}/\lambda^3$, with $\lambda = \frac{G}{\eta}(4\pi)^{1/3}$, where G is the growth rate of the extended grain. In the equation above I_0, considered constant, is the nucleation rate comprehensive of phantoms, that is for uncorrelated nuclei throughout the entire space (as

defined in the KJMA model).

Fig. 3a shows the normalized nucleation rate, $Q_a(\bar{t})$, for several values of $\beta = \beta'\eta/G$. It was calculated using Eq. (2), as described in the previous section and in the Supplementary Material (Eq. (S11) in Supplementary Material), by appropriately selecting the spatial integration domains (Fig. 2). The nucleation rate $Q_{a,K}(\bar{t})$ given by the KJMA approach, Eq. (13), is also reported as dashed line in Fig. 3. Note that Eq. (2) describes a stochastic process of correlated nuclei, and this also applies to $\beta = 0$ according to Eq. (11). In fact, actual nuclei are always correlated since nucleation of actual nuclei is only allowed in the untransformed phase. It should be noted that for $\beta = 0$ the result of Eqs. (2), (S11) (open symbols in Fig. 3a) is in excellent agreement with the KJMA model, for which, thanks to the inclusion of phantoms, the nuclei in the entire space are not correlated. This result supports the validity of the second-order approximation used in the present approach.

As anticipated in section 2.3.1 the difference between Q_a and $Q_{a,K}$ is due to the overgrowth of phantoms which render some portions of the untransformed phase unavailable for nucleation (see Fig. 1b). The difference $\Delta Q_a(\bar{t}) = Q_a(\bar{t}) - Q_{a,K}(\bar{t})$ is reported in Fig. 3b; it is representative of the relative variation of the nucleation rates with respect to I_0. The relative variation of the number density of actual nuclei, $\frac{\Delta n_a}{n_a} = \left(\int_0^\infty Q_a d\bar{t}\right)^{-1} \int_0^\infty \Delta Q_a d\bar{t}$, is lower than 5% for β values up to 0.6 to increase up to 20% for $\beta = 1$. This provides a measure of the goodness of the approximation given by Eq. (13).

From the knowledge of the actual nucleation rate the volume fraction of the transformed phase, $V(\bar{t})$, can be estimated through Eq. (2) (and Eq. (S10) in the Supplementary Material) by considering the spatial integration domains depicted in Fig. 2. The results are displayed in Fig. 4 for different values of β. It follows that the kinetics of V slows down as β increases. Increasing β brings two opposite effects into play; on the one hand a reduction of the impingement events among crystals (nuclei are more isolated) should lead to an increase of the transformed volume, while on the other hand a decrease in the nucleation rate of actual nuclei should decrease the transformed volume. The computation of Fig. 4 indicates a slightly greater effect of the nucleation rate compared to impingement. A similar effect on the transformed volume kinetics has also been reported in ref. [27] but for a different pair correlation function.

As reported above, the key quantity to determine the actual volume of the growing crystal is the conditional probability $P_c(t|t_1)$ that enters Eq. (5b). This probability was calculated using Eq. (8), further elaborated in Eq. (S14) in the Supplementary Material. For the sake of simplicity, in the following we discuss the results for $\beta = 0.4$, although the $P_c(t|t_1)$ probability was calculated for several values of β to model the crystal-size PDFs reported below.

Fig. 5a displays $P_c(\bar{t}|\bar{t}_1)$ as a function of $\bar{t}$ for several values of $\bar{t}_1$ and

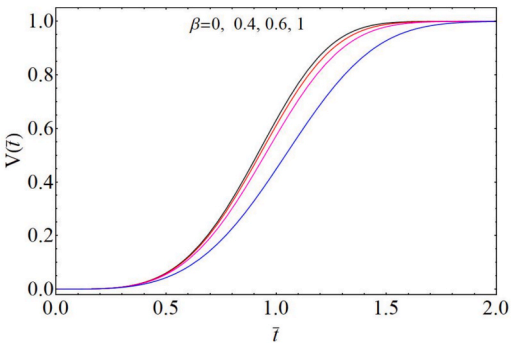

Fig. 4. Time dependence of the fraction of transformed volume for different values of β. In the graphs, at a given time the volume decreases as the correlation degree, β, increases.

for $\beta = 0.4$. In the figure, the dashed lines represent the conditional probabilities for the KJMA model ($\beta = 0$) given by Eq. (6) and for the same values of $\bar{t}_1$. The probability P_c is defined for $t \geq t_1$, being equal to one for $t = t_1$. In the graphs the greater $\bar{t}_1$ the greater the shift of the curve toward longer times. Compared to the P_c curves of the KJMA model, those at $\beta \neq 0$ are shifted toward longer times. At $\beta \neq 0$, $P_c(\bar{t}|\bar{t}_1)$ is equal to one in a finite interval of time $\Delta\bar{t}$. This behavior is due to the delay in the impingement between crystals caused by the spatial correlation. According to Eq. (11) the distance between two nucleation centers cannot be shorter than β'. Consequently, the first collision event between two nuclei with birth times t_1 and $t_2 < t_1$ and linear growth occurs when the radii satisfy the equation: $R(t_1 - t_2) + \beta' = R(t - t_1) + R(t - t_2)$ with solution $R(t - t_1) = \beta'/2$. Furthermore, we recall the definition of $P_c(t|t_1)$ as the probability that, given the formation of an actual nucleus at time t_1, the point at distance $R(t - t_1)$ remains untransformed up to time t. Based on the previous computation we deduce that a generic point at distance $r = R(t - t_1)$ remains untransformed up to time t provided that $R(t - t_1) \leq \beta'/2$. The point at distance $\beta'/2$ is untransformed by either grains up to reduced time $(\bar{t} - \bar{t}_1) = \frac{\beta}{2}$. Therefore $P_c(\bar{t}|\bar{t}_1) = 1$ up to $\bar{t} = \bar{t}_1 + \frac{\beta}{2}$. In fact, for the curves of Fig. 5a $\Delta\bar{t} = \frac{\beta}{2} = 0.2$.

The $P_c(\bar{t}|\bar{t}_1)$ probability has also been calculated using Eqs. (8),(S14 in Supplementary Material) based on the correlation function approach, for KJMA transformations at $\beta = 0$. Noteworthy, these results are in excellent agreement with the exact analytical solution given by Eq. (6) as shown in Fig. 5b. This result also supports the second-order approximation used in Eq. (8).

The growth kinetics of the actual crystals, namely the mean volume as a function of running time and birth time of nuclei, has been calcu-

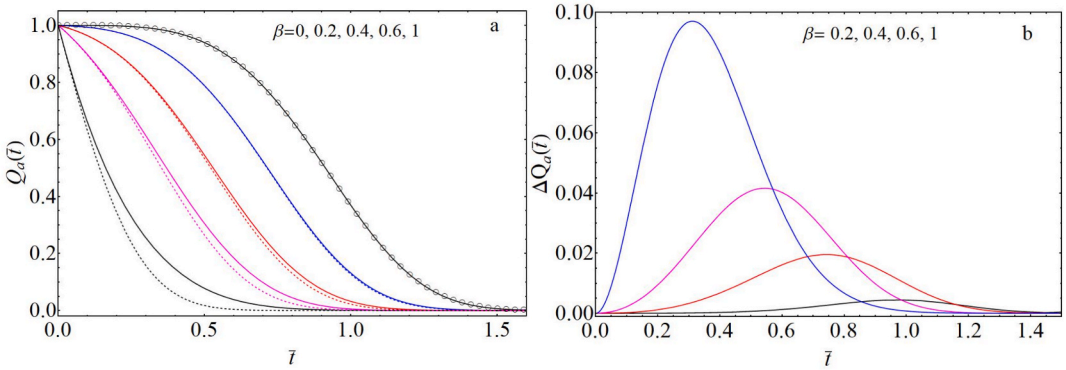

Fig. 3. Panel a): Kinetics of formation of actual nuclei with time dependent hard-sphere correlation according to Eqs. (2),(11) (solid lines for $\beta \neq 0$ and open symbols for $\beta = 0$). The parameter β is a measure of the correlation strength between nuclei. The higher β the lower $Q_a(\bar{t})$. The $Q_{a,K}(\bar{t})$ curves calculated using the KJMA approach are also shown as dashed lines for $\beta > 0$ and as solid line for $\beta = 0$. Panel b): The difference between the actual nucleation rates given by Eq. (2) and Eq. (13) are shown for several values of β. Nucleation rates have been normalized to I_0.

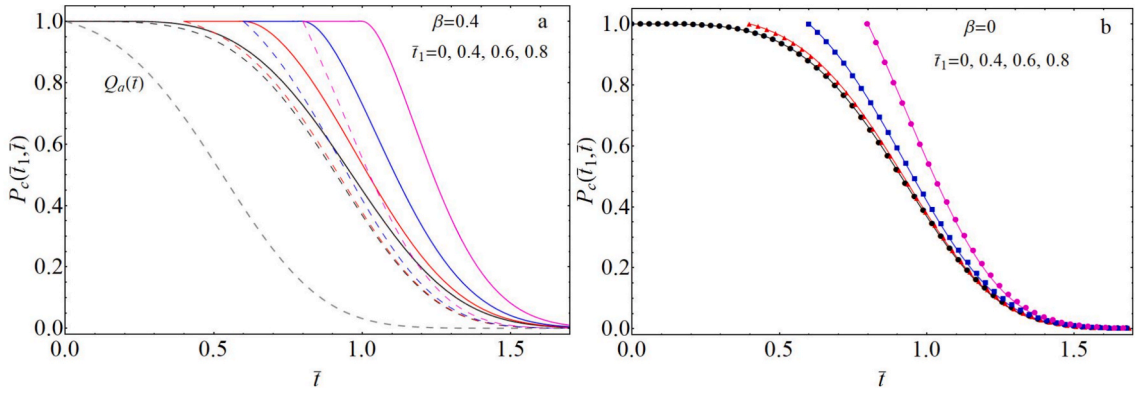

Fig. 5. Panel a): $P_c(\bar{t}|\bar{t}_1)$ probability for several values of $\bar{t}_1$ at $\beta = 0.4$ (full lines). Dashed lines are the P_c probabilities for the KJMA approach, Eq. (6), for the same values of $\bar{t}_1$. The nucleation rate is also reported as dashed line. Panel b): The $P_c(\bar{t}|\bar{t}_1)$ probability, calculated using the correlation function approach (Eq. (8) and Eq. (S14) in Supplementary Material) at $\beta = 0$, is shown as solid symbols and compared with the exact solution Eq. (6) (solid line).

lated by integrating $P_c(\bar{t}|\bar{t}_1)$ in Eq. (5b) (see also Eq. (S1) in Supplementary Material). These kinetics are reported in Fig. 6a as solid lines and are compared to the evolution of the mean volume in KJMA growths. For $\beta = 0$ and linear growth in 3D, the KJMA model yields the analytical solution given by Eq. (7) according to [14]

$$v(\bar{t},\bar{\tau}) = \frac{1}{4}e^{\bar{\tau}^4}\left(\bar{\tau}^2\,\Gamma\left(\frac{1}{4},\bar{\tau}^4,\bar{t}^4\right) - 2\bar{\tau}\Gamma\left(\frac{2}{4},\bar{\tau}^4,\bar{t}^4\right) + \Gamma\left(\frac{3}{4},\bar{\tau}^4,\bar{t}^4\right)\right), \tag{14}$$

where $\Gamma(a,z_0,z_1)$ is the generalized incomplete gamma function.[5] The $v(\bar{t},\bar{\tau})$ values calculated using the approach based on correlation functions at $\beta = 0$, are in excellent agreement with Eq. (14). The mean volume for the case $\beta \neq 0$ is greater than that at $\beta = 0$. This is due to the reduction in the density of actual nuclei and impingent events between grains in the correlated case, which implies less constrained growth when compared to the KJMA transformation.

Let us now consider, at running time t, the contribution to the transformed volume of actual nuclei with birth times in the interval $0 \leq \tau \leq \tau_c$ (with $\tau_c \leq t$). This contribution is equal to $V_{\bar{t}}(\bar{\tau} \leq \bar{\tau}_c) = \frac{1}{K(\bar{t})}\int_0^{\bar{\tau}_c} I_a(z)v(\bar{t},z)dz$, with $K(\bar{t}) = \int_0^{\bar{t}} I_a(z)v(\bar{t},z)dz$. In Fig. 6b the behavior of $V_{\bar{t}}(\bar{\tau} \leq \bar{\tau}_c)$ is shown as solid line for a nearly complete transformation, i.e. for $V(\bar{t}) = 0.99$.These computations indicate that the most significant contribution to the transformed volume is due to nucleation events occurring in the early stage of the phase transition. The horizontal line at $V = 0.9$ and the $V(\bar{\tau}_c)$ kinetics, in dashed lines, highlight the low value of the transformed volume at time $\bar{\tau}_c$ such that actual nuclei born up to $\bar{\tau}_c$ provide 90% of the whole transformed volume.

The knowledge of $I_a(\bar{t})$ and $v(\bar{t},\bar{\tau})$ allows us to determine the PDF of crystal volume by using Eq. (10c). The PDF, at the end of the transformation ($V = 0.99$), are shown in Fig. 7a for different values of β. Compared to the KJMA distribution ($\beta = 0$), the main feature of the PDF at $\beta \neq 0$ is the change in both peak intensity and position. There is a marked reduction in the intensity of the PDF peak, shifting to higher volume values with increasing correlation. Moreover, with increasing β the PDF becomes more uniform and the maximum size of the crystals increases with β. In Fig. 7b the PDF at $\beta = 0$, computed using the correlation function approach, is compared to the analytical solution obtained using Eqs. (10c),(13) and (14). Even for this quantity, the agreement between the two approaches is very good.

Finally, let us consider another model system of correlated nucleation in 3D transformations, in which nucleation is excluded in a sphere of radius $r_c = \alpha R$, encompassing the grain, with constant $\alpha \geq 1$. In this case the radius of the correlation sphere is equal to $r_c(t_1,t_2) = \alpha R(t_1 - t_2)$. In addition, since for this system there is no overgrowth of phantoms, the rate of formation of actual nuclei is given by the KJMA kinetics:

$$Q_a(\bar{t}) = e^{-\alpha^3\bar{t}^4}. \tag{15}$$

Fig. 8a shows the trend of Q_a for different values of α calculated using the correlation function method with Q_a given by Eq. (15). As Fig. 8a shows, the results of Eq. (2) are in very good agreement with Eq. (15). The PDF of the grain size at the end of the transformation ($V = 0.99$) is shown in Fig. 8b. Compared to the other case discussed above (i.e. with a constant shell size, β), the PDF resembles a step function that is more extended as α increases. For both hard-sphere correlations considered

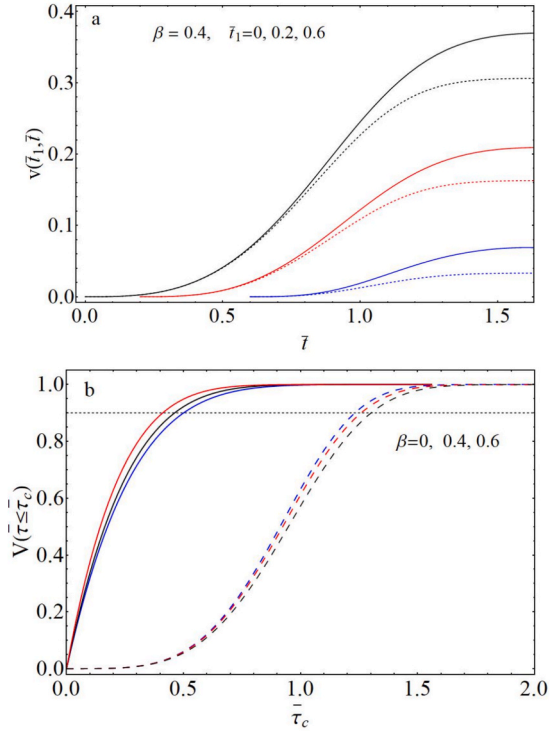

Fig. 6. Panel a): Mean volume of the actual nuclei as a function of time, for several values of nucleus birth time, $\bar{t}_1$. The dashed lines are the mean volumes for $\beta = 0$, according to Eq. (14). Panel b): Contribution, to the volume fraction of a nearly complete transformation, due to actual crystals with birth times in the range $[0,\bar{\tau}_c]$ (solid lines). The evolution of the volume fraction of the new phase is displayed as dashed line. Computations refer to $\beta = 0, 0.4, 0.6$ where, at given $\bar{\tau}_c$, $V(\bar{\tau} \leq \bar{\tau}_c)$ increases with β.

[5] The generalized incomplete gamma function is defined as $\Gamma(a,z_0,z_1) = \int_{z_0}^{z_1} x^{a-1}e^{-x}dx$. Furthermore, $\Gamma(a) \equiv \Gamma(a,0,\infty)$.

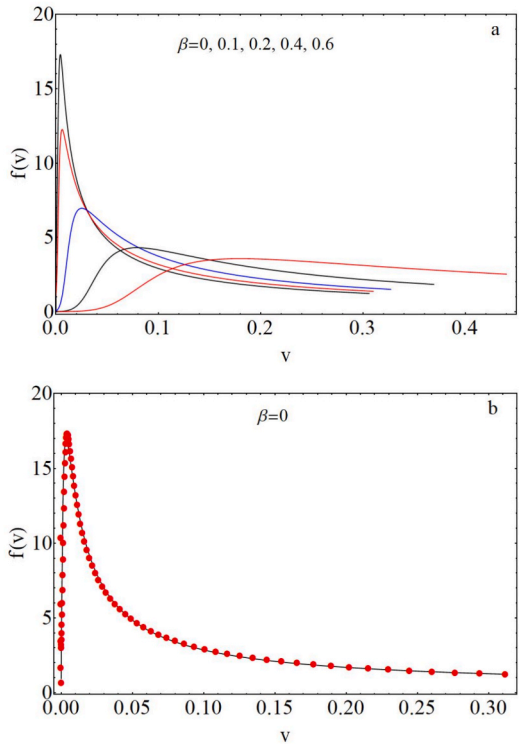

Fig. 7. Panel a): Probability density function of crystal size for different values of the correlation parameter, β. As β increases, the peaks shift toward higher volumes and decrease in intensity. Panel b): Comparison between the PDF at $\beta = 0$ computed using the correlation function approach (symbols) and the solution obtained by the KJMA model (solid line).

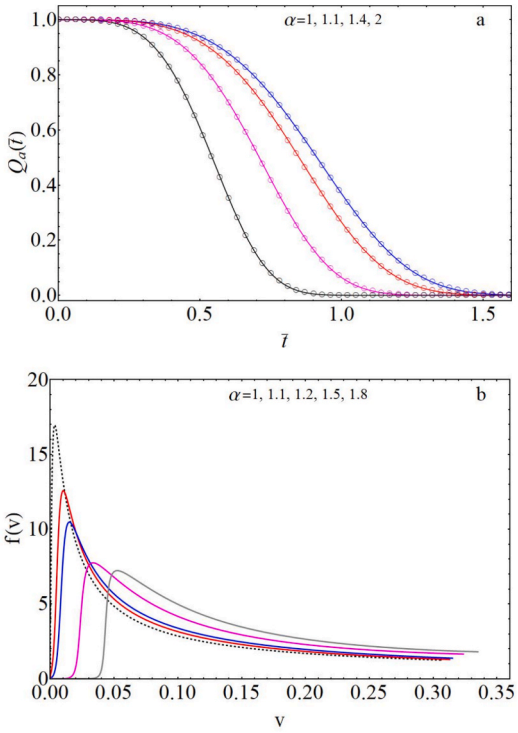

Fig. 8. Nucleation rate of the actual nuclei (Panel a)) and PDF of the grain size (Panel b)) for hard-sphere correlation with radius $r_c(t_1, t_2) = \alpha R(t_1 - t_2)$ and $\alpha \geq 1$. In Panel a), the numerical computations obtained from Eq. (2) and Eq. (12) are shown as symbols for different values of α, where the solid line is the nucleation rate given by the KJMA model, Eq. (15). At given $\bar{t}$, Q_a decreases with α. The PDF shifts towards larger values of v as α increases.

here, the absence of crystal populations with low values of v is due to the sharp decrease of nucleation rate with time, as α or β increases and to the behavior of the $\partial_\tau v(t,\tau)$ derivative. It is worth noting that, according to the meaning of P_c in Eq. (5b), $v(t,\tau)$ is the volume the τ-crystal would have at time t given that it started growing between τ and $\tau + d\tau$. It follows that, even though Eq. (5b) provides a finite volume for a class of τ-crystals, these may not contribute significantly to the PDF due to the negligible nucleation rate at τ. The situation is illustrated in Fig. 9 for the cases $\alpha = 1.8$ and the KJMA approach ($\alpha = 1$). In the figure, the nucleation rate of actual nuclei and the $v(\bar{t},\bar{\tau})$ at $V(\bar{t}) = 0.99$, are displayed. In the case $\alpha = 1.8$ when Q_a is extremely small, $\partial_{\bar{\tau}} v \neq 0$ which implies $f(v) \cong 0$ (inset of Fig. 9). Conversely, for $\alpha = 1$, when $\partial_{\bar{\tau}} v$ is very small, Q_a is non-zero leading to large values of $f(v)$ in Eq. (10c).

An issue related to the transformation kinetics concerns the effect of the finite volume of the critical nucleus, $v_0 \equiv \bar{v}(t,t) = v_{ex}(t,t)$. This implies adding in the equations for the rate $\partial_t \xi(t)$ and the growth law $\bar{v}(t,\tau)$ the extra terms $I_a(t)v_0$ and, v_0, respectively. Since the $\partial_{\bar{\tau}}\bar{v}$ derivative is not substantially altered by this change, the effect on the PDF (Eq. (10c) is essentially a translation of the function by v_0. It follows that the relevant length scales to evaluate such an effect are the size of the critical nucleus (R_c) and the average value of nucleus population. With reference to the PDF for completed transformation, as reported in this section, these two length scales yield the product $q = R_c n^{1/3}$ as an indicator for the approximation $v_0 \approx 0$. Typical values for R_c and n in the solid state fall in the range $1 - 10nm$ and $10^{12} - 10^{15} nuclei/m^3$ respectively [33]. The q parameter is in the range $10^{-3} - 10^{-5}$ providing support for the assumption of vanishing initial volume.

Before concluding, it is worth noting that, to the best of the author's knowledge, a direct comparison with experimental results is currently not possible due to the lack of 3D data on phase transitions meeting the model's conditions. Nevertheless, the validity of the correlation-function-based approach can be verified through computer simulations, an example of which is provided in the Supplementary Materials. Moreover, as discussed in the Supplementary Material, the numerical results of this section offer insight on how to apply the model in conjunction with experimental data on nucleation density and PDF.

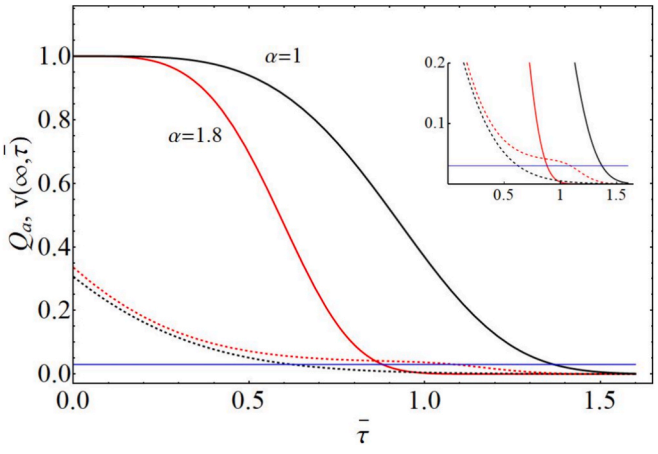

Fig. 9. Nucleation rate (solid line) and mean volume of τ-crystals when transition is completed (dashed line), as a function of $\bar{\tau}$. The kinetics refer to the KJMA transition (i.e. $\alpha = 1$, black curves) and to correlated nuclei with $\alpha = 1.8$ (red curves). The straight horizontal line at $v = 0.03$ marks the onset point of $f(v)$ for $\alpha = 1.8$ (Fig. 8a). Inset: detail of the trends of the crystal volume (dashed lines) and nucleation rate (solid lines). (For interpretation of the references to colour in this figure legend, the reader is referred to the web version of this article.)

3. Conclusions

We propose a correlation-function-based method for modeling the mean size of actual crystals in phase transformations with correlated nuclei. The approach allows determining the nucleation rate of actual nuclei, the mean volume of τ-crystals at running time t and the transformed volume fraction. From the nucleation rate and mean volume of crystal the PDF is eventually computed. The method is applied to the case of hard-sphere correlation with either a constant or time dependent shell around the crystals, within which nucleation is forbidden. In the former case, owing to phantom overgrowth, the nucleation rate is obtained by solving an integral equation, while in the latter the KJMA model applies. The case of KJMA compliant transformations (where nuclei forms at random in the untransformed portion of space) can be equally well studied using the actual nucleation rate within the correlation function approach. This is a useful approach to assess the validity of the second-order approximation employed here. In fact, the good consistency between the two approaches for the quantities reported above supports the use of this approximation. For both types of correlated nucleations the presence of the shell in which nucleation is prevented leads to a drastic decrease in nucleation rate with time and a shift of the PDF toward higher crystal volumes. Furthermore, for low values of v the PDF is almost zero in a region that is wider the greater the correlation.

CRediT authorship contribution statement

Massimo Tomellini: Writing – original draft, Methodology, Formal analysis, Conceptualization.

Declaration of competing interest

The author declare that they have no known competing financial interests or personal relationships that could have appeared to influence the work reported in this paper.

Appendix A. Supplementary data

Supplementary data to this article can be found online at https://doi.org/10.1016/j.jcrysgro.2026.128675.

Data availability

Data will be made available on request.

References

[1] A.N. Kolmogorov, On the statistical theory of the crystallization of metals, URSS Bull. Acad. Sci. (Cl. Sci. Math. Nat.) 3 (1937) 355–359.
[2] W.A. Johnson, R.F. Mehl, Reaction kinetics in processes of nucleation and growth, Trans. AIME 135 (1939) 416–458.
[3] M. Avrami, Kinetics of phase change. I General theory, J. Chem. Phys. 7 (1939) 1103–1112.
[4] J.S. Blazquez, F.J. Romero, C.F. Conde, A. Conde, A Review of different models derived from classical Kolmogorov, Johnson and Mehl and Avrami (KJMA) theory to recover physical meaning in solid-state transformations, Phys. Status Solidi (b) 259 (2022) 2100524.
[5] B. Rheingans, E.J. Mittemeijer, Phase transformation kinetics: advanced modeling strategies, JOM 65 (9) (2013) 1145–1154.
[6] K. Shirzad, C. Viney, A critical review on application of the Avrami equations beyond materials science, J. R. Soc. Interface 20 (2023) 20230242.
[7] J. Vázquez, C. Wagner, P. Villares, R. Jimenez-Garay, A theoretical method for determining the crystallized fraction and kinetic parameters by DSC, using non-isothermal techniques, Acta Mater. 44 (1996) 4807–4813.
[8] R.A. Ramos, P.A. Rikvold, M.A. Novotny, Test of the Kolmogorov-Johnson-Mehl-Avrami picture of metastable decay in a model with microscopic dynamics, Phys. Rev. B 59 (1999) 9053–9069.
[9] P. Bruna, D. Crespo, R. Gonzàlez-Cinca, On the validity of Avrami formalism in primary christallization, J. Appl. Phys. 100 (2006) 054907.
[10] E. Pineda, P. Bruna, D. Crespo, Cell size distribution in random tessellations of space, Phys. Rev. E 70 (2004) 066119.
[11] A.V. Teran, A. Bill, R.B. Bergmann, Time evolution of grain size distribution in random nucleation and growth crystallization process, Phys. Rev. B 81 (2010) 075319.
[12] M. Tomellini, Interface evolution in phase transformations ruled by nucleation and growth, Phys. A 558 (2020) 124981.
[13] V.G. Dubrovskii, Fluctuation-induced spreading of size distribution in condensation kinetics, J. Chem. Phys. 131 (2009) 164514.
[14] M. Tomellini, On the grain size distribution function in KLMA compliant growth, J. Cryst. Growth 584 (2022) 126579;
M. Tomellini, Fokker-Planck equation for the particle size distribution function in KJMA transformations, Physica A 615 (2023) 128515;
M. Tomellini, M. De Angelis, Fokker-Planck equation for the crystal-size probability density in progressive nucleation and growth with application to lognormal, Gaussian and gamma distributions, J. Cryst. Growth 650 (2025) 127970.
[15] D.A. Barlow, J. Gregus, Size evolution and composition of the intermediate phase during nonclassical protein crystal growth from solution, Cryst. Growth Design 20 (2020) 4959–4966.
[16] M.J. Rost, L. Jacobse, M.T.M. Koper, Non-random island nucleation in the electrochemical roughening on Pt(111), Angew. Chem. Int. Ed. 62 (2023) e202216376.
[17] L. Guo, P.C. Searson, Simulations of island growth and island spatial distribution during electrodeposition, Electrochem. Solid-State Lett. 10 (2007) D76–D78.
[18] G.E. Moehl, P.N. Bartlett, A.L. Hector, Using GISAXS to detect correlations between the locations of gold particles electrodeposited from an aqueous solution, Langmuir 36 (2020) 4432–4438.
[19] Y. Sun, G. Zangari, Observation of Weibull, lognormal, and gamma distributions in electrodeposited Cu and Cu-Ag particles, Materials 16 (2023) 6452.
[20] M. Tomellini, Spatial distribution of nuclei in progressive nucleation, Phys. A: Stat. Mech. and Its Appl. 496 (2018) 481–494.
[21] A.P. Grinin, F.M. Kuni, Y.S. Djikaev, Statistico-probabilistic approach to taking account of the vapor depletion in the kinetics of homogeneous nucleation: a free-molecular regime of droplet growth, J. Chem. Phys. 120 (4) (2004) 1846–1854.
[22] A.E. Kuchma, A.K. Shchekin, D.S. Martyukova, Nucleation stage of multicomponent bubbles of gases dissolved in a decompressed liquid, J. Chem. Phys. 148 (2018) 234103.
[23] M. Tomellini, M. Fanfoni, M. Volpe, Spatially correlated nuclei: how the Johnson-Mehl-Avrami-Kolmogorov formula is modified in the case of simultaneous nucleation, Phys. Rev. B 62 (2000) 11300–11303.
[24] W.S. Tong, J.M. Rickman, K. Barmak, Impact of short-range repulsive interactions between nuclei on the evolution of a phase transformation, J. Chem. Phys. 114 (2001) 915–922.
[25] E. Pineda, T. Pradell, D. Crespo, Non-random nucleation and the Avrami kinetics, Philos. Mag. A Phys. Condens. Matter, Struct. Defects Mech. Prop. 82 (2002) 107–121.
[26] J.M. Rickman, K. Barmak, Kinetics of first order phase transitions with correlated nuclei, Phys. Rev. E 95 (2017) 022121.
[27] M. Tomellini, Nucleation kinetics in phase transformations with spatially correlated nuclei, Phys. A 676 (2025) 130882.
[28] M. Tomellini, M. Fanfoni, Comparative study of approaches based on the differential critical region and correlation functions in modeling phase transformation kinetics, Phys. Rev. E 90 (2014) 052406.
[29] N.G. Van Kampen. Stochastic Processes in Physics and Chemistry, North Holland Publishing Company, Amsterdam, New York, Oxford, 1981.
[30] N.V. Alekseechkin, Extension of the Kolmogorov–Johnson–Mehl–Avrami theory to growth laws of diffusion type, J. Non Cryst. Solids 357 (2011) 3159–3167.
[31] J.P. Hansen, I.R. McDonald. Theory of Simple Liquids, 2nd ed., Academic Press, London, 1986.
[32] M.P. Shepilov, Kinetics of transformation for a model with the diffusion law of growth of new-phase particles nucleated on active centers, Glas. Phys. Chem. 30 (4) (2004) 291–299.
[33] V.I. Savran, S.E. Offerman, J. Sietsma, Austenite nucleation and growth observed on the level of individual grains by three-dimensional X-ray diffraction microscopy, Metall. Mater. Trans. A 41A (2010) 583–591.